

Novel Route to Faster Fourier Transform Infrared Spectroscopic Imaging

ROHIT BHARGAVA, MICHAEL D. SCHAEBERLE, DANIEL C. FERNANDEZ,* and IRA W. LEVIN†

Laboratory of Chemical Physics, National Institute of Diabetes and Digestive and Kidney Diseases, National Institutes of Health, Bethesda, Maryland 20892-0510

Fourier transform infrared (FT-IR) spectroscopic imaging microscopy couples a focal plane array (FPA) detector, integrated within an infrared microscope assembly, to an interferometer for attaining a multiplex/multichannel signal detection advantage. While this configuration should enable the acquisition of spatially resolved spectra over the entire field of view of a sample in the time that it takes a conventional FT-IR spectrometer to record a single spectrum, data acquisition in an imaging modality is an intrinsically slower process. We present a novel collection technique for step-scan, micro-imaging spectrometers that both allows large numbers of samples to be imaged rapidly and provides higher signal-to-noise ratios (SNRs) for given experimental time intervals. For example, data may be collected in as little as one minute, while SNRs greater than 800 are achieved for data acquired in less than 10 min. Imaging data acquired in the proposed, more rapid approach exhibit no loss in fidelity compared to data recorded by the conventional imaging techniques.

Index Headings: FT-IR; Imaging; Focal plane array; Signal-to-noise ratio; Hyperspectral data cube; Step-scan; Continuous scan; Rapid scan; Data collection; Trigger method.

INTRODUCTION

Infrared imaging of microscopic samples using focal plane array (FPA) detection techniques became feasible through the coupling of an FPA to both a Fourier transform infrared (FT-IR) spectrometer and an IR microscope.^{1,2} This technique has been used in analyzing polymer composites^{3,4} and blends,⁵ liquid crystal polymeric systems,^{6,7} and polymer diffusion,⁸ as well as in the examination of tissue sections from humans,^{9–11} mice,¹² rats,¹³ and monkeys,² and samples of food grains.¹⁴ In comparison to conventional microspectroscopic (namely, mapping) instrumentation, it is apparent that a major advantage of infrared spectroscopic imaging is the large reduction in the experimental time required for acquiring high fidelity data.¹⁵ The combination of spectral multiplexing, which is inherent to the interferometer, and FPA multichannel detection should allow spatially resolved spectra to be collected over the entire field of view being sampled in the time that it takes to collect data from microspectroscopic instrumentation equipped with solely single element detection. FT-IR imaging, however, represents an intrinsically slower modality for collecting an interferogram compared to the single element detector system. The additional time required for data acquisition is primarily due to the poor signal-to-noise ratio (SNR)

characteristics of FPAs and the longer readout and storage times required for accessing thousands of individual detector elements.

It is well recognized that a reduction in data collection times adds power to this imaging technique, making it even more widely applicable to the areas of materials and biological research. Faster data collection can be achieved either by shorter readout and storage times or by reducing noise characteristics through the improvement of associated hardware. Hardware advances, however, are rare, expensive, and usually untenable alternatives to existing instrumentation. Noise reduction may also be achieved through post-collection techniques, where improvement in the SNR of the processed data is dependent on the SNR of the unprocessed data.^{16,17} These techniques require additional computation time and may not be universally applicable to specific experimental scenarios. Devising efficient collection strategies for noise reduction by analyzing the details of the collection process becomes a highly desirable approach toward increasing the SNR of data collected in a specific experimental time period.

To devise an efficient collection strategy, it is instructive to understand the mechanism of data collection for commonly used step-scan instrumentation. In the interferometer, optical retardation remains constant for a given time before being stepped sequentially to evenly spaced retardation positions (Fig. 1). For every retardation step, the FPA is synchronized to collect a number of image frames, which are subsequently averaged and stored in a computer as the image corresponding to that retardation. An analysis for the SNR obtained from FPAs based on the collection parameters in this process is given by¹⁸

$$SNR_{FPA} = \left[\frac{U_v(T) \left(2\pi A (1 - \sqrt{1 - (NA)^2}) \right) \Delta\bar{\nu} \xi \delta_{FPA}}{\frac{\sqrt{A_D}}{D^*}} \epsilon_c (n_i t)^{1/2} \right] \quad (1)$$

where $U_v(T)$ is the spectral energy density at a given wavenumber, A_D the detector area, and D^* the specific detectivity. The throughput is given by the imaged sample area (A) and the light intensity is determined by optics associated with a numerical aperture, NA . $\Delta\bar{\nu}$ is the spectral resolution and ξ is the spectrometer efficiency. The efficiency of the microscope equipped with an FPA is given by δ_{FPA} , ϵ_c is the acquisition ratio, n_i the number of image cubes collected, and t is the time required to collect one image cube. The acquisition ratio, defined as

Received 27 March 2001; accepted 30 April 2001.

* Howard Hughes Medical Institute—National Institutes of Health Research Scholar.

† Author to whom correspondence should be sent.

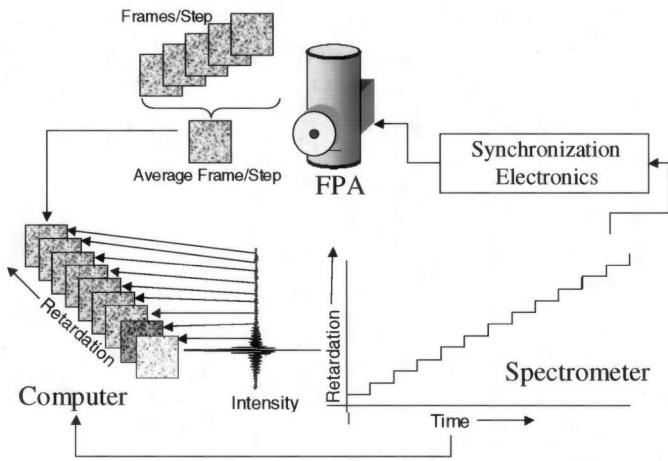


FIG. 1. Schematic of the setup for an infrared imaging system using an FPA and a step-scan interferometer. The spectrometer is stepped to achieve a retardation and the FPA is triggered to collect data. Upon stabilization of the interferometer retardation, the FPA collects data and all collected frames are read off to the computer to be averaged before the next spectrometer step is triggered. Data are available as a hyper-spectral data cube with signals at known retardations (interferograms) for every pixel or an image per retardation.

the ratio of array staring time to the total time per step, was found to reasonably predict the achieved SNR.¹⁸ Assuming the time for constant retardation to be optimal, the acquisition ratio is given by

$$\epsilon_c = \frac{n_f t_I}{t_d + n_f t_f + t_r} \quad (2)$$

where n_f is the maximum number of frame co-adds allowable at the spectrometer stepping rate, t_I is the integration time per frame of time period t_f , t_d represents the

time delay to allow the spectrometer to stabilize, and t_r provides the time required to read out, average, and store the FPA frame data for the retardation step. The efficiency of data collection is greatly reduced when data obtained only for a small fraction of the total frame time and a large “dead time” is allowed for spectrometer stabilization, reading the array, and storing of data. The fraction of frame time used for integration and readout, determined by the array characteristics, is fixed by the manufacturer. Since the time required by the spectrometer to achieve a specific retardation can also be assumed to be fixed, there appears to be little flexibility for further improvement in the data collection process.

PROPOSAL

In this manuscript, we propose a new method for collecting data that will increase the acquisition ratio, ϵ_c , and lead to a more efficient and faster data collection protocol. The data collection process in an imaging setup can be considered to originate from a continuous electrical trigger output from the interferometer electronics (Fig. 2a). This internal signal generator is used to provide periodic pulses, or triggers, which change the spectrometer retardation at a determined rate. The pulse, with a time period t_p , is usually tens of microseconds in duration. Once the electrical trigger steps the mirror(s) in the interferometer to achieve a sequential retardation, the mirror(s) move and stabilize in time t_d . This settling time is fairly constant from step to step and run to run and is of the order of tens of milliseconds. The same internal trigger is split and fed to the FPA electronics. FPA data collection is initiated after a time delay to allow the interferometer mirror(s) to stabilize at each retardation position. Since the interferometer retardation is constant, the

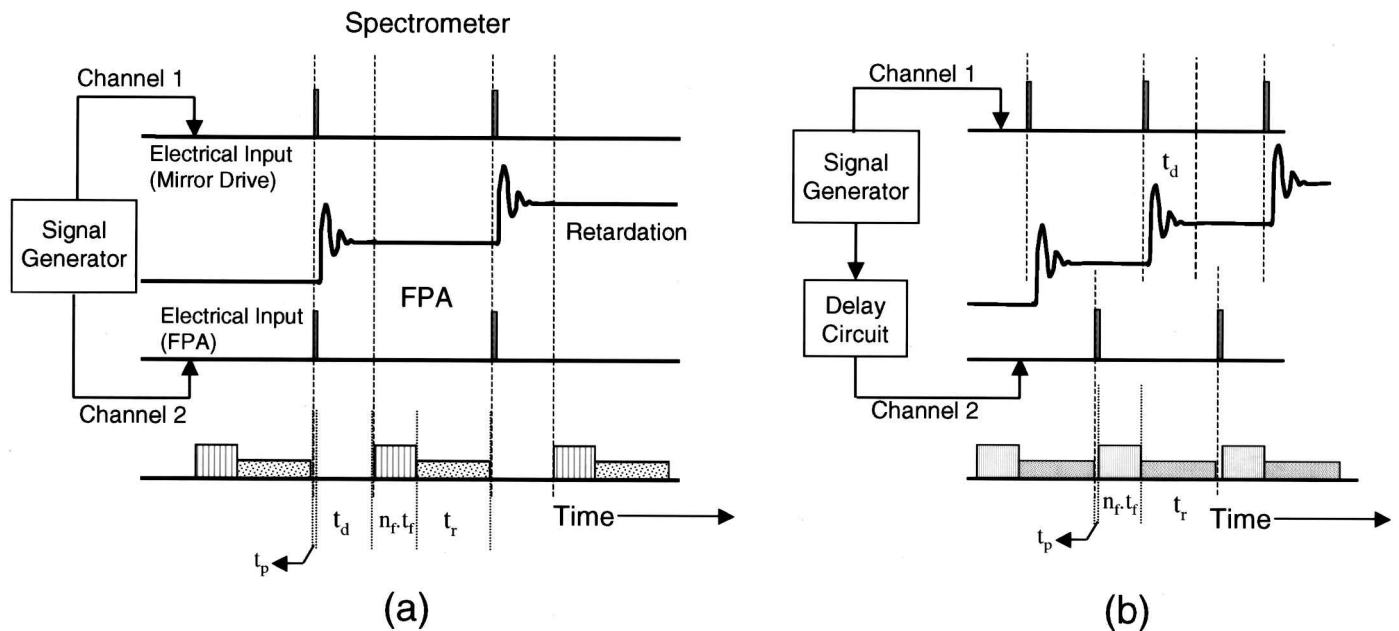


FIG. 2. (a) Data collection using the conventional collection scheme. A timed signal generator is used to trigger spectrometer steps by an electrical pulse ($t_p \sim 50 \mu\text{s}$), the interferometer mirrors stabilize ($t_d \sim 40 \text{ms}$) and data are collected over the next interval of time given by the product of the number of frames (n_f) and time for each frame (t_f). The data are read and stored while the spectrometer retardation is maintained (t_r). (b) A delay circuit is incorporated into the electrical path before the trigger is fed to the FPA input. The FPA is triggered after the spectrometer has stabilized and collects data as in (a). The array is read and stored while the spectrometer is stepped and stabilized.

array detector collects data for a time given by the product of the number of frames (n_f) and frame time (t_f); the data are then read and stored in the computer in time t_r . The internal signal generator then sends out another trigger pulse, and the process is repeated for the desired number of steps.

The above process of data collection has achieved widespread implementation and works well; however, it also results in significant dead times. If the control center of the instrument is considered to be an independent signal generator rather than an interferometer timing clock, the interferometer and the FPA are then independently controlled. It is clear that during the interferometer mirror(s) stepping and stabilization stages, the FPA is idle. Further, during the FPA readout and storage stages, the interferometer remains idle. While seemingly interdependent and sequential, these two events (interferometer stepping and FPA readout) are actually independent processes, and the time required for the two steps may be combined into one step to achieve higher efficiency. That is, while the interferometer is performing the step process, the array is read and stored. Thus, the larger of t_d and t_r in Eq. 3 determines the total dead time for the process.

IMPLEMENTATION

The implementation of the above concept is shown schematically in Fig. 2b. The interferometer is stepped, using electrical triggers as in the conventional implementation, with the same trigger being split to another output for the FPA. A delay circuit is incorporated between this output and the trigger input to the FPA, with the delay time set to be larger than the time required for mirror stabilization. As seen in the figure, the FPA collects data when the interferometer assumes a stable retardation. While the array data for that step is being read and stored, the interferometer is stepped to the next retardation in the sequence. During the stabilization of the interferometer, the reading of the array is completed and the FPA is triggered for collection at the new retardation. Using this technique, data can be collected more rapidly without loss of spectral or spatial fidelity.

EXPERIMENTAL

A step-scan spectrometer (Bruker IFS 66/s) is interfaced to an IR microscope (Bruker IR Scope II) with an FPA (Santa Barbara Focalplane) at the distal end of the optical train. The FPA detector is a 64×64 pixel MCT array equipped with an optimally sized cold shield and appropriate bandpass filters. The sensitivity of the detector is a spectral window from 2.3 to 11 microns (~ 4000 – 900 cm^{-1}), which images a sample area of $\sim 500 \mu\text{m} \times 500 \mu\text{m}$. Single-sided collection yielded a total of 4096 interferograms, one for each detector element. Five hundred and twelve data points are collected at an undersampling ratio of 4 to yield spectra with a resolution of approximately 16 cm^{-1} over a 0 – 3950 cm^{-1} range. This interferogram data cube is fast Fourier transformed using triangular apodization.

For the conventional imaging implementation, 40 and 95 ms are provided as delay and readout times, respectively. Twenty image frames are co-added after being col-

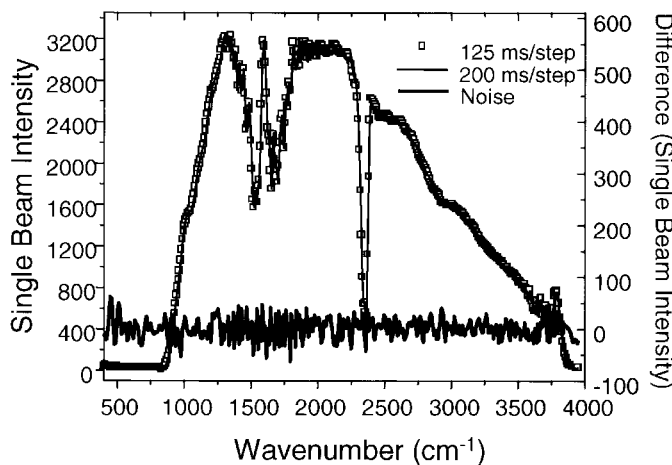
lected at a frame rate of 315.1 Hz (integration time of 0.099 ms per frame). Thus, the total time allowed for frame acquisition is 65 ms. With a holding time at each optical retardation point of 200 ms, we achieve a total collection time of 103 s for each data set. For the proposed implementation, the interferometer trigger is fed to the FPA and delayed for 40 ms. Data are collected over the subsequent 65 ms. Data readout to the computer was then immediately initiated. A time delay of 20 ms is allowed after data collection before again triggering the interferometer. Thus, the total time between spectrometer triggers is 125 ms, resulting in a collection time of less than 65 s for the image cube. The interferometer is usually triggered by a pulse with tens of μs , which is negligible compared to the other times involved and is, therefore, neglected.

A thin ($\sim 10 \mu\text{m}$) film of polystyrene (ICI plc) was sandwiched between two BaF_2 flats (Wilmad). The assembly was placed in the beam path, and the microscope was focused using the film edge-air interface between the substrates. Background image data sets were acquired from areas approximately 1 mm outside the film, while film images were recorded approximately 1 mm inside the boundary. The FPA was flat fielded prior to data acquisition with the use of a two-intensity calibration of the radiation intensity passing through the microscope optics. No diffuser was used. The sample and background single beam data cubes were ratioed pixel-by-pixel in the conversion to an absorbance image data cube. Matlab (Mathworks Inc.) and ENVI (Research Systems Inc.) provided platforms for software written in-house for data extraction and computation.

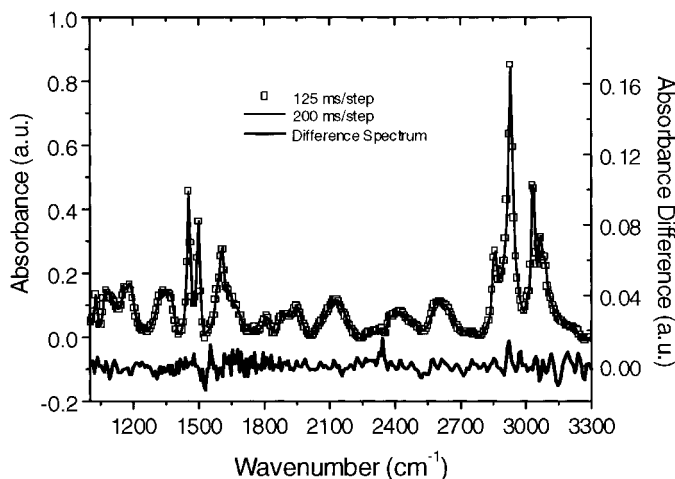
RESULTS AND DISCUSSION

The proposed collection scheme was successfully implemented. The camera readout time, t_r , was systematically varied to find the minimum time for stable interferometer/FPA operation. Using too small a time period results in a triggering of the camera before the FPA readout is complete, leading to either communication failure between the computer and the FPA or a loss in the initiation of data collection at subsequent retardation steps. Thus, the collection process may either fail or some retardation point(s) may not be sampled, leading to spectral distortions. For our instrumentation, we were able to obtain reliable readout and storage characteristics for a single image in less than 60 ms/step. The total collection time was 65 s, which compares favorably to a collection time of 103 s using the conventional scheme. If only a single frame of data is collected per step, the total collection time for an image cube is approximately 35 s. This compares favorably with times obtained by fast collection of data using rapid scan interferometry,¹⁹ but with the present method providing the step-scan interferometric advantage of retardation stability.

An important test of the proposed implementation is to determine whether the fast data collection scheme results in inferior SNR data. A single beam spectrum extracted from a randomly chosen pixel is compared to a spectrum from the same pixel at two different rates of data collection (Fig. 3a). The data from the conventional collection scheme (200 ms/step) and from the fast col-



(a)



(b)

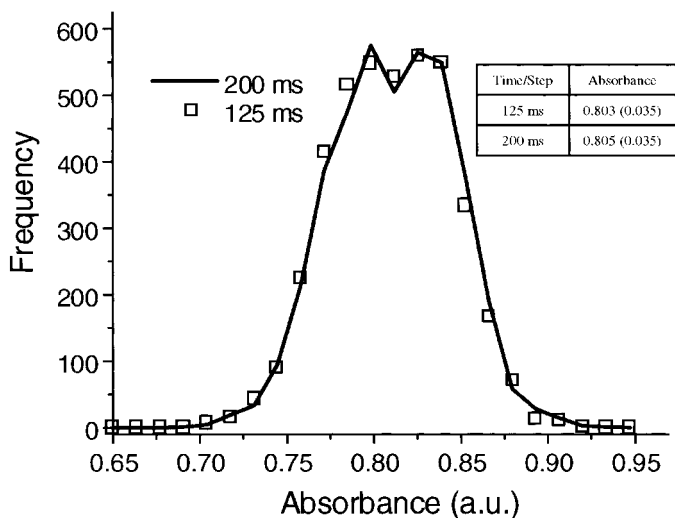
FIG. 3. (a) A comparison of the single beam spectra obtained from a single pixel using the conventional detection scheme (200 ms/step) and the proposed collection scheme (125 ms/step). The scale for the difference of the single beam intensities is indicated on the right ordinate and is one-fifth the magnitude of the single beam intensity scale on the left ordinate. (b) A comparison of the absorbance spectra obtained from a single pixel using the conventional detection scheme (200 ms/step) and the proposed collection scheme (125 ms/step) and their difference spectrum. The scale for the difference of the absorbance spectra is indicated on the right axis and is one-fifth the magnitude of the absorbance spectra scale on the left axis. (c) A comparison of the absorbance distribution of the asymmetric CH_2 stretching absorbance (2929 cm^{-1}) using the conventional detection scheme (200 ms/step) and the proposed collection scheme (125 ms/step). The insert shows the average absorbance and standard deviation (in parenthesis) for both cases.

lection scheme (125 ms/step) under the same collection conditions differ only by noise. A difference spectrum between the two single beam spectra shows no spectral features above the noise level. Possible noise arising from spikes or high/low frequency noise in the interferogram should be easily seen as corresponding Fourier transform features in the difference spectrum. No evidence for increased noise or periodic perturbations were found in an examination of the difference spectra from the two data sets.

Absorbance spectra of a thin polystyrene film were also similar, differing only in noise (Fig. 3b). Baseline fringes in the absorbance spectrum are due to the constant thickness film sandwiched between the two salt plates. The fringes are faithfully reproduced in both data sets, precluding the possibility of their origin from any noise sources due to fast data collection. The difference spectrum is featureless, implying no loss of fidelity. A plot of the distribution of the aliphatic asymmetric CH_2 stretching mode absorbance ($\sim 2929 \text{ cm}^{-1}$) over the film obtained using the two collection schemes is shown in Fig. 3c. The absorbance distributions are identical. Fringing in the sample gives the distribution an appearance of two populations and a distribution width larger than that due to noise alone. This finding can be readily verified by plotting a non-absorbing frequency close to the peak and observing the same pattern.

The efficiency of data collection for imaging systems may be determined by the acquisition ratio, which is a measure of the fractional collection time per step while radiation intensity is being detected. With current detector

FIG. 3. Continued.



(c)

FIG. 3. Continued.

technology, the collection efficiency for imaging systems is 1% given the large stabilization, readout, and storage times. In the new collection scheme, the stabilization time is concurrent with the readout and storage times; hence, the acquisition ratio is larger. The improvement can be seen as a function of co-added frames in Fig. 4. The relative advantage, plotted in the insert of Fig. 4, is determined by a ratio of the acquisition ratios of the smaller time per step to the larger time per step. The benefits can be seen to decrease as the number of co-added frames increases due to the decreasing contribution of the total “dead” time as a fraction of the time spent at each retardation. Thus, for rapid data collection using 1 frame, the efficiency is 70% greater, while for the usual collection conditions (20 frames), an improvement of 40% is expected.

A smaller time required for data collection for every image cube implies that the SNR obtained by time av-

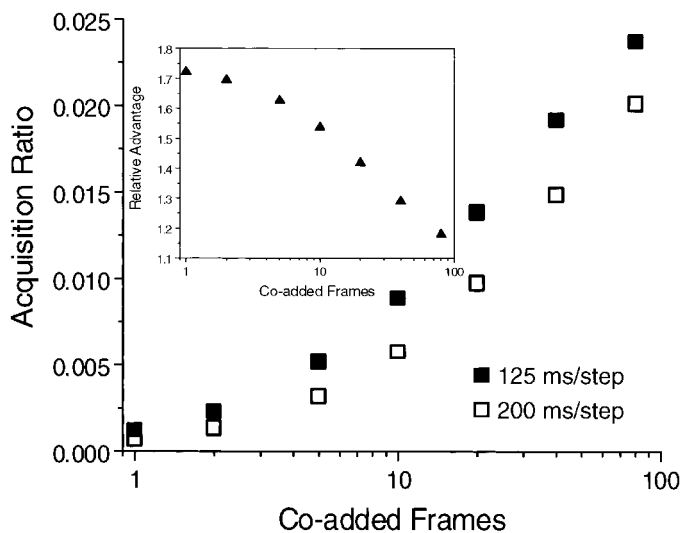


FIG. 4. A comparison of the acquisition ratio using the conventional detection scheme (200 ms/step) and the proposed collection scheme (125 ms/step). The insert shows the relative advantage of the new collection scheme.

eraging multiple data cubes is also more efficient. It has been shown that the optimal number of frames for the highest SNR is usually close to 20.¹⁸ For a data collection process co-adding 20 frames per image set, the resulting SNR possible as a function of time using both the conventional method and the more rapid collection scheme is shown in Fig. 5. Data are presented that are normalized to the SNR for one image cube and then extrapolated using a square root dependence of SNR on the number of co-added image data sets. The advantages of fast collection times become increasingly pronounced as more images are averaged. A typical SNR for a spectrum extracted from a single pixel in a single image cube collected in a matter of minutes is ~ 300 . Based on the variation of the SNR with numbers of co-added image sets, a reasonable collection time of 10 minutes/sample will yield a SNR of ~ 675 using the old scheme compared to ~ 825 for the new approach. A 20 minute collection for the same conditions would yield a SNR of ~ 1200 using the new scheme, as opposed to a SNR of ~ 975 . This technique also facilitates the treatment of data using derivative spectral techniques and curve resolution methods. The increase in sensitivity by achieving desired figures of merit (detection limits and quantification levels) in a shorter time is apparent. Further, the faster data acquisition method enhances the capability of the experimentalist to monitor dynamic processes in real-time. For example, assuming that the change in concentration during data acquisition is over no more than a single pixel, diffusion processes with a linear velocity of $\sim 7.5 \mu\text{m}/\text{min}$ may be measured compared to a limit of $\sim 4.5 \mu\text{m}/\text{min}$ using the conventional mode of data acquisition.

We have proposed the implementation of a generalized, staggered step-scan approach. Other implementations are also possible. In the present implementation, there is no feedback from when the data is read and stored to when the spectrometer is triggered for the next step. Incorporation of such feedback allows for a more robust system, but requires complicated electronics and programming. An external trigger generator may be used

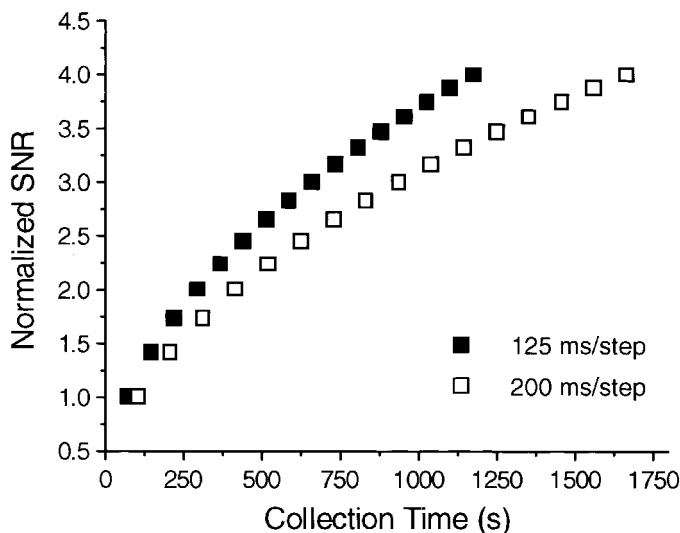


FIG. 5. A comparison of the SNR of spectra from a single pixel using the conventional detection scheme (200 ms/step) and the proposed collection scheme (125 ms/step) normalized to the SNR of data collected at 20 frames for a single image cube.

for an independent triggering of the two components based on their internal clocks; however, such an arrangement is more prone to failure if the interferometer has small variations in its stepping rate. The methodology presented in this manuscript offers a convenient and easy route for staggered triggering.

CONCLUSION

A new collection scheme is proposed to conduct FT-IR imaging experiments with the use of an FPA and a step-scan interferometer. A substantial reduction in the collection time per image cube is obtained. This approach allows either the examination of more samples in a given experimental time or permits an increased SNR by time averaging more efficiently. A comparison of data obtained in the analysis of the same polymer sample showed little difference between the results obtained from a conventional single element detector and the fast image collection scheme. The proposed methodology allows for more efficient data collection and more effective signal averaging to improve the SNR. Signal-to-noise ratios of over 800 should be readily achievable for most systems in less than 10 minutes of collection time. Lastly, the proposed scheme is easy to implement and is quite robust.

1. E. N. Lewis, P. J. Treado, R. C. Reeder, G. M. Story, A. E. Dowrey, C. Marcott, and I. W. Levin, *Anal. Chem.* **67**, 3377 (1995).
2. E. N. Lewis, A. M. Gorbach, C. Marcott, and I. W. Levin, *Appl. Spectrosc.* **50**, 263 (1996).
3. J. M. Chalmers, N. J. Everall, K. Hewitson, M. A. Chesters, M. Pearson, A. Grady, and B. Ruzicka, *Analyst (Cambridge, U.K.)* **123**, 579 (1998).
4. M. van der Weert, R. van't Hof, J. van der Weerd, R. M. A. Heeren, G. Posthuma, W. E. Hennink, and D. J. A. Crommelin, *J. Controlled Release* **68**, 31 (2000).
5. C. M. Snively and J. L. Koenig, *J. Polym. Sci., Part B: Polym. Phys.* **37**, 2353 (1999).
6. R. Bhargava, S-Q. Wang, and J. L. Koenig, *Macromolecules* **32**, 2748 (1999).

7. R. Bhargava, S-Q. Wang, and J. L. Koenig, *Appl. Spectrosc.* **52**, 323 (1998).
8. C. M. Snively and J. L. Koenig, *J. Polym. Sci., Part B: Polym. Phys.* **37**, 2261 (1999).
9. L. H. Kidder, V. F. Kalasinsky, J. L. Luke, I. W. Levin, and E. N. Lewis, *Nature Medicine* **3**, 235 (1997).
10. C. Marcott, R. C. Reeder, E. P. Paschalis, A. L. Boskey, and R. Mendelsohn, *Phosphorus Sulfur* **146**, 417 (1999).
11. R. Mendelsohn, E. P. Paschalis, and A. L. Boskey, *J. Biomed. Optics* **4**, 14 (1999).
12. E. N. Lewis, L. H. Kidder, P. Pentchev, I. W. Levin, and D. S. Lester, *Biophys. J.* **72**, MPME5 (1997).
13. E. N. Lewis, I. W. Levin, J. P. Hanig, and D. S. Lester, *Biophys. J.* **70**, WP180 (1996).
14. C. Marcott, R. C. Reeder, J. A. Sweat, D. D. Panzer, and D. L. Wetzel, *Vib. Spectrosc.* **19**, 123 (1999).
15. R. Bhargava, B. G. Wall, and J. L. Koenig, *Appl. Spectrosc.* **54**, 470 (2000).
16. R. Bhargava, T. Ribar, and J. L. Koenig, *Appl. Spectrosc.* **53**, 1313 (1999).
17. R. Bhargava, S-Q. Wang, and J. L. Koenig, *Appl. Spectrosc.* **54**, 486 (2000).
18. R. Bhargava and I. W. Levin, *Anal. Chem.*, paper submitted.
19. C. M. Snively, S. Katzenberger, G. Oskarsdottir, and J. Lauterbach, *Opt. Lett.* **24**, 1841 (1999).